Two-Step Spin Conversion for the Three-Dimensional Compound Tris(4,4′-bis-1,2,4-triazole)iron(II) Diperchlorate

Yann Garcia,† Olivier Kahn,*,† Louis Rabardel,† Benoit Chansou,‡ Lionel Salmon,‡ and Jean Pierre Tuchagues*,‡

Laboratoire des Sciences Moléculaires, Institut de Chimie de la Matière Condensée de Bordeaux, UPR CNRS No. 9048, 33608 Pessac, France, and Laboratoire de Chimie de Coordination, UPR CNRS No. 8241, 31077 Toulouse, France

Received May 11, 1999

The title compound, $[Fe(btr)_3](ClO_4)_2$, has been synthesized. The investigation of its magnetic properties has revealed a low-spin ↔ high-spin conversion occurring in two steps, each step involving 50% of the Fe^{2+} ions. The low-temperature step is very abrupt and occurs with a thermal hysteresis whose width is about 3 K around $T_1 = 184$ K. The high-temperature step, centered around $T_2 = 222$ K, is rather gradual. Differential scanning calorimetric measurements have confirmed the occurrence of a two-step spin conversion. The enthalpy and entropy variations associated with the two steps have been found as $\Delta H_1 = 5.7$ kJ mol^{-1} and $\Delta S_1 = 30.1$ J mol^{-1} K^{-1}, and $\Delta H_2 = 6.5$ kJ mol^{-1} and $\Delta S_2 = 28.6$ J mol^{-1} K^{-1}, respectively. The crystal structure of $[Fe(btr)_3](ClO_4)_2$ has been solved at three temperatures, namely, above the high-temperature step (260 K), between the two steps (190 K), and below the low-temperature step (150 K). The compound crystallizes in the trigonal system, space group $R\bar{3}$, at the three temperatures. The structure is three-dimensional. There are two Fe^{2+} sites, denoted Fe1 and Fe2. Each of them is located on a 3-fold symmetry axis and an inversion center and is surrounded by six btr ligands through the nitrogen atoms occupying the 1- or 1′-positions. Each btr ligand bridges an Fe1 and an Fe2 site, with an Fe1−Fe2 separation of 8.67 Å at 260 K. The perchlorate anions are located in the voids of the three-dimensional architecture and are hydrogen bonded to the triazole rings of the btr ligands. These anions do not interact with the Fe1 and Fe2 sites exactly in the same way. At 260 K, both the Fe1 and Fe2 sites are high-spin (HS) with Fe−N bond lengths of 2.161(3) and 2.164(3) Å, respectively. At 190 K, the Fe1 site remains HS while the Fe2 site is low-spin (LS) with Fe−N bond lengths of 2.007(3) Å. Finally, at 150 K, both the Fe1 and Fe2 sites are LS with Fe−N bond lengths of 1.987(5) and 1.994(5) Å, respectively. It turns out that the two-step spin conversion is associated with the presence of two slightly different Fe^{2+} sites. The spin conversion regime has also been followed by Mössbauer spectroscopy. These findings have been discussed and compared to the previously reported cases of two-step spin conversions.

Introduction

One of the very appealing aspects of the phenomenon of spin conversion between high-spin (HS) and low-spin (LS) states resides in the occurrence of bistability, i.e., the possibility to observe two electronic states in a given range of external perturbation.[1−4] For Fe^{2+} compounds, these states are characterized by the spin quantum numbers $S = 2$ and $S = 0$.[5−11] For an assembly of spin crossover molecules governed by the thermodynamical regime, the perturbation may be the temperature, and then bistability leads to the occurrence of thermal hysteresis, which endows the system with a memory effect.[1] It is now well established that the interaction between spin crossover sites within the crystal lattice is one of the key factors governing the bistability, and in the past few years endeavors have been carried out to design spin crossover compounds exhibiting strong intersite interactions. Along this line, two strategies are currently explored, namely, the supramolecular approach and the polymeric approach.[12] The former strategy consists of imposing strong intermolecular interactions between mononuclear spin crossover species, using the tools of supramolecular chemistry.[13−15] The latter strategy consists of linking together the spin crossover sites by chemical bridges into extended or polymeric structures.[16] So far, one- and two-dimensional spin

† UPR CNRS No. 9048.
‡ UPR CNRS No. 8241.

(1) Kahn, O.; Launay, J. P. *Chemtronics* **1988**, *3*, 140.
(2) Zarembowitch, J.; Kahn, O. *New J. Chem.* **1991**, *15*, 181.
(3) Kahn, O. *Molecular Magnetism*; VCH: New York, 1993.
(4) Kahn, O. *Curr. Opin. Solid State Mater. Sci.* **1996**, *1*, 547.
(5) Goodwin, H. A. *Coord. Chem. Rev.* **1976**, *18*, 293.
(6) Gütlich, P. *Struct. Bonding (Berlin)* **1981**, *44*, 83.
(7) König, E.; Ritter, G.; Kulshreshtha, S. K. *Chem. Rev.* **1985**, *85*, 219.
(8) König, E. *Prog. Inorg. Chem.* **1987**, *35*, 527.
(9) Gütlich, P.; Hauser, A. *Coord. Chem. Rev.* **1990**, *97*, 1.
(10) König, E. *Struct. Bonding (Berlin)* **1991**, *76*, 51.
(11) (a) Gütlich, P.; Hauser, A.; Spiering, H. *Angew. Chem., Int. Ed. Engl.* **1994**, *33*, 2024 and references therein. (b) Gütlich, P.; Jung, J.; Goodwin, H. A. In *Molecular Magnetism: from Molecular Assemblies to the Devices*; Coronado, E., Delhaès, P., Gatteschi, D., Miller, J. S., Eds.; NATO ASI Series C, Vol. 321; Kluwer Academic: Dordrecht, 1996; p 327. (c) Gütlich, P. *Mol. Cryst. Liq. Cryst.* **1997**, *305*, 17.
(12) Kahn, O.; Garcia, Y.; Létard, J. P.; Mathonière, C. In *Supramolecular Engineering of Synthetic Metallic Materials. Conductors and Magnets*; Veciana, J., Rovira, C., Amabilino, D. B., Eds.; NATO ASI Series C, Vol. 518; Kluwer Academic Publishers: Dordrecht, 1998; p 127.
(13) Létard, J. P.; Guionneau, P.; Codjovi, E.; Lavastre, O.; Bravic, G.; Chasseau, D.; Kahn, O. *J. Am. Chem. Soc.* **1997**, *119*, 10861.
(14) Zhong, Z. J.; Tao, J. Q.; Yu, Z.; Dun, C. Y.; Liu, Y. J.; You, X. Z. *J. Chem. Soc., Dalton Trans.* **1998**, 327.
(15) Létard, J. F.; Guionneau, P.; Rabardel, L.; Howard, J. A. K.; Goeta, A. E.; Chasseau, D.; Kahn, O. *Inorg. Chem.* **1998**, *37*, 4432.

10.1021/ic990511q CCC: $18.00
Published on Web 09/29/1999

crossover compounds have been reported.[17−32] Some of them exhibit abrupt transitions along with wide thermal hysteresis, up to ca. 40 K.[22] Most of these compounds incorporate 1,2,4-triazole-type ligands. On the other hand, to the best of our knowledge, no three-dimensional spin crossover compound has been described so far.

In this paper, we report on the first three-dimensional spin crossover compound and explore its structural and physical properties. The formula of the compound is $[Fe(btr)_3](ClO_4)_2$, where btr stands for 4,4′-bis-1,2,4-triazole, whose structure is recalled hereunder: [33]

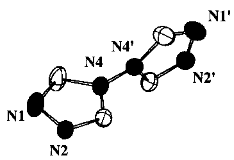

The btr molecule, which was already used in the field of spin conversion compounds, is known to be able to bridge Fe^{2+} ions through the nitrogen atoms occupying the 1- and 1′-positions.[18,19] $[Fe(btr)_3](ClO_4)_2$ exhibits a thermally induced spin conversion occurring in two steps. To analyze this behavior in a thorough manner, we will describe the crystal structures at three different temperatures, namely, 260, 190, and 150 K. We will also investigate the magnetic and thermodynamical properties of the compound, as well as the temperature dependence of the Mössbauer spectra. Finally, we will compare the two-step spin conversion observed for this compound to the other cases reported so far where the spin conversion also occurs in two steps.

(16) Kahn, O.; Jay Martinez, C. *Science* **1998**, *279*, 44.
(17) Lavrenova, L. G.; Ikorskii, V. N.; Varnek, V. A.; Oglezneva, I. M.; Larionov, S. V. *Koord. Khim.* **1986**, *12*, 207; **1990**, *16*, 654.
(18) Vreugdenhil, W.; van Diemen, J. H.; de Graaff, R. A. G.; Haasnoot, J. G.; Reedgijk, J.; van der Kraan, A. M.; Kahn, O.; Zarembowitch, J. *Polyhedron* **1990**, *9*, 2971.
(19) Ozarowski, A.; Shunzhong, Y.; McGarvey, B. R.; Mislankar, A.; Drake, J. E. *Inorg. Chem.* **1991**, *30*, 3167.
(20) Kahn, O.; Kröber, J.; Jay, C. *Adv. Mater.* **1992**, *4*, 718.
(21) Sugiyarto, K. H.; Goodwin, H. A. *Aust. J. Chem.* **1994**, *47*, 263.
(22) Kröber, J.; Audière, J. P.; Claude, R.; Codjovi, E.; Kahn, O., Haasnoot, J. G.; Grolière, F.; Jay, C.; Bousseksou, A.; Linarès, J.; Varret, F.; Gonthier-Vassal, A. *Chem. Mater.* **1994**, *6*, 1404.
(23) Lavrenova, L G.; Ikorskii, V. N.; Varnek, V. A.; Oglezneva, I. M.; Larionov, S. V. *Polyhedron* **1995**, *14*, 1333.
(24) Real, J. A.; Andrés, E.; Muñoz, M. C.; Julve, M.; Granier, T.; Bousseksou, A.; Varret, F. *Science* **1995**, *268*, 265.
(25) Bronisz, R.; Ciunik, Z.; Drabent, K.; Rudolf, M. F. *Conf. Proc., ICAME-95* **1996**, *50*, 15.
(26) Kitaziwa, T.; Gomi, Y.; Takahashi, M.; Takeda, M.; Enomoto, M.; Miyazaki, A.; Enoki, T. *J. Mater. Chem.* **1996**, *6* (1), 119.
(27) Bronisz, R.; Drabent, K.; Polomka, P.; Rudolf, M. F. *Conf. Proc., ICAME-95* **1996**, *50*, 11.
(28) Kahn, O.; Codjovi, E.; Garcia, Y.; van Koningsbruggen, P. J.; Lapouyade, R.; Sommier, L. In *Molecule-Based Magnetic Materials*; Turnbull, M. M., Sugimoto, T., Thompson, L. K., Eds.; ACS Symposium Series 644; American Chemical Society: Washington, DC, 1996.
(29) Garcia, Y.; van Koningsbruggen, P. J.; Codjovi, E.; Lapouyade, R. L.; Kahn, O.; Rabardel, L. *J. Mater. Chem.* **1997**, *7* (7), 857.
(30) van Koningsbruggen, P. J.; Garcia, Y.; Codjovi, E.; Lapouyade, R. L.; Kahn, O.; Fournès, L.; Rabardel, L. *J. Mater. Chem.* **1997**, *7* (7), 2069.
(31) Garcia, Y.; van Koningsbruggen, P. J.; Lapouyade, R. L.; Rabardel, L.; Kahn, O.; Wierczorek, M.; Bronisz, R.; Ciunik, Z.; Rudolf, M. F. *C. R. Acad. Sci. Paris* **1998**, *11c*, 523.
(32) Garcia, Y.; van Koningsbruggen, P. J.; Lapouyade, R.; Fournès, L.; Rabardel, L.; Kahn, O.; Ksenofontov, V.; Levchenko, G.; Gütlich, P. *Chem. Mater.* **1998**, *10*, 2426.
(33) Domiano, P. *Cryst. Struct. Commun.* **1977**, *6*, 503.

Experimental Section

Synthesis. The ligand 4,4′-bis-1,2,4-triazole, hereafter abbreviated as btr, was synthesized as previously described.[34] $[Fe(btr)_3](ClO_4)_2$ was prepared as follows: A solution containing 0.40 g (2.94 mmol) of btr dissolved in a mixture of 5 mL of water and 5 mL of methanol and warmed to 60 °C was added to a solution containing 0.35 g (0.96 mmol) of $[Fe(H_2O)_6](ClO_4)_2$ and 2 mg of ascorbic acid dissolved in 10 mL of water, and also warmed to 60 °C. Single crystals of the desired material were obtained by slow evaporation at room temperature within 1 week. Anal. Calcd for $C_{12}H_{12}N_{18}Cl_2O_8Fe$: C, 21.74; H, 1.82; N, 38.02; Cl, 10.69; Fe, 8.42. Found: C, 21.69; H, 1.89; N, 36.76; Cl, 10.72; Fe, 8.27.

Magnetic Measurements. These were carried out with a DSM-8 susceptometer working in the 4.2−300 K temperature range. Magnetic data were corrected for magnetization of the sample holder and for diamagnetic contributions, which were estimated from Pascal's constants.

Calorimetric Measurements. These were carried out with a Perkin-Elmer DSC-7 differential scanning calorimeter working down to 100 K. The compound was sealed in an aluminum sample holder. Temperatures and enthalpies were calibrated using the two crystal−crystal transitions of a pure cyclopentane sample (122.0 K, 4871 J mol^{-1}, and 131.8 K, 346.5 J mol^{-1}). The temperatures were determined with a $\pm$0.1 K accuracy, and the uncertainty on the enthalpy values was estimated as $\pm$0.1 kJ mol^{-1}. The experiment was carried out in a He gas atmosphere. The heating and cooling rates were fixed at 2 K min^{-1}.

Crystallographic Data Collection and Structure Determination. A selected crystal of $[Fe(btr)_3](ClO_4)_2$ was mounted on a Stoe imaging plate diffraction system (IPDS) equipped with an oxford cryosystems cooler device. Three temperatures were investigated, namely, 260, 190, and 150 K. Unit cell dimensions with esd's were obtained from least-squares refinement of 5000 reflections. Crystal decay was monitored by measuring 200 reflections per image. Crystallographic data and other pertinent information are summarized in Table 1. The structure was solved by direct methods using SIR92[35] and subsequent difference Fourier maps. The calculations were carried out with the CRYSTALS package programs running on a PC.[36] Atomic form factors for neutral atoms were taken from ref 37. Corrections were made for Lorentz and polarization effects, and a numerical absorption correction was applied.[38] A Chebyshev weighting scheme was used.[39] All hydrogen atoms were found on difference Fourier syntheses and refined. Anisotropic temperature factors were introduced for all non-hydrogen atoms. Full-matrix least-squares refinements were carried out by minimizing the function $\sum w(||F_o| - |F_c||)^2$ where F_o and F_c are the observed and calculated structure factors. The model reached convergence with $R = \sum(||F_o| - |F_c||)/\sum|F_o|$ and $R_w = [\sum w(||F_o| - |F_c||)^2/\sum w(|F_o|)^2]^{1/2}$ having values listed in Table 1. Figures 3−5 were drawn with the CAMERON software.[40]

^{57}Fe Mössbauer Measurements. Mössbauer measurements were obtained on a constant-acceleration conventional spectrometer with a 25 mCi source of ^{57}Co (Rh matrix). Isomer shift values (δ) are given with respect to metallic iron at room temperature. The absorber was a sample of 120 mg of microcrystalline powder enclosed in an 18 mm diameter cylindrical plastic sample holder, the size of which had been determined to optimize the absorption. Variable-temperature spectra

(34) Haasnoot, J. G.; Groeneveld, W. L. *Z. Naturforsch.* **1979**, *34b*, 1500.
(35) Altomare, A.; Cascarano, G.; Giacovazzo, G.; Guagiardi, A.; Burla, M. C.; Polidori, G.; Camalli, M. SIR92 a Program for Automatic Solution of Crystal Structures by Direct Methods. *J. Appl. Crystallogr.* **1994**, *27*, 435.
(36) Watkin, D. J.; Prout, C. K.; Carruthers, R. J.; Betteridge, P. *Crystals*, issue 10; Chemical Crystallography Laboratory: Oxford, England, 1996.
(37) *International Table for X-Ray Crystallography*; Kynoch Press: Birmingham, England, 1994; Vol. IV.
(38) *X-SHAPE, Crystal Optimisation for Numerical Absorption Correction*, version 1.01; STOE & Cie GmbH: Darmstadt, Germany, 1996.
(39) Carruthers, J. R.; Watkin, D. J. *Acta Crystallogr.* **1979**, *A35*, 698.
(40) Watkin, D. J.; Prout, C. K.; Pearce, L. J. *Cameron*; Chemical Crystallography Laboratory, University of Oxford: Oxford, England, 1996.

Table 1. Crystallographic Data for $[Fe(btr)_3](ClO_4)_2$ at 260, 190, and 150 K

formula	$C_{12}H_{12}Cl_2O_8FeN_{18}$	$C_{12}H_{12}Cl_2O_8FeN_{18}$	$C_{12}H_{12}Cl_2O_8FeN_{18}$
mol wt	663	663	663
temp (K)	260	190	150
space group	$R\bar{3}$ (No. 148)	$R\bar{3}$ (No. 148)	$R\bar{3}$ (No. 148)
a, b (Å)	10.9708(8)	10.9379(8)	10.030(1)
c (Å)	35.517(4)	34.555(3)	33.008(4)
α, β (deg)	90	90	90
γ (deg)	120	120	120
V (Å^3)	3702.0(4)	3580.2(4)	3477.5(4)
Z	6	6	6
ρ_{calc} (g/cm^3)	1.78	1.85	1.90
μ (Mo Kα, cm^{-1})	9.4	9.35	9.63
$R(F)^a$	0.040	0.038	0.072
$R_w(F^2)^a$	0.045	0.042	0.079

[a] $R(F) = \sum||F_{obs}| - |F_{calc}||/\sum|F_{obs}|$; $R_w(F^2) = [\sum w(|F_{obs}| - |F_{calc}|)^2/\sum w|F_{obs}|^2]^{1/2}$; $w = w'(1 - [\Delta F/6\sigma(F)]^2)^2$ and $w' = \sum(r = 1,x)\mathrm{ArTr}(x)$, where Ar are the coefficients for the Chebyshev polynomial Tr(x) with $x = F_{calc}/F_{calc(max)}$.

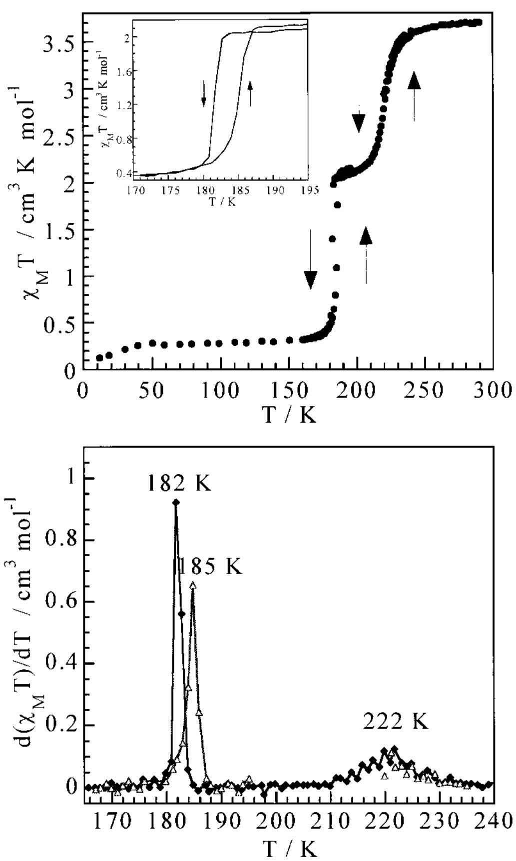

Figure 1. (top) Temperature dependence of $\chi_M T$ for $[Fe(btr)_3](ClO_4)_2$. The inset emphasizes the thermal hysteresis for the low-temperature step of the spin conversion. (bottom) Temperature dependence of the derivatives $d(\chi_M T)/dT$ in both the cooling and warming modes and determination of the inversion temperatures (see text).

were obtained in the 300−80 K range by using a MD 306 Oxford cryostat, the thermal scanning being monitored by an Oxford ITC4 servocontrol device. The accuracy on the temperature was ±0.1 K. A least-squares computer program was used to fit the Mössbauer parameters and determine their standard deviations of statistical origin (given in parentheses).[41]

Magnetic Properties

The magnetic properties of the compound are represented in Figure 1 (top) in the form of the $\chi_M T$ versus T curve, χ_M being the molar magnetic susceptibility and T the temperature. Let us recall that in a first approximation the high-spin molar fraction, x_{HS}, is given by[3]

$$x_{HS} = \chi_M T/(\chi_M T)_{HT} \qquad (1)$$

where $(\chi_M T)_{HT}$ is the high-temperature limit of $\chi_M T$. Equation 1 assumes that the molar magnetic susceptibility for the compound in the HS state follows the Curie law.

At room temperature, $\chi_M T$ is equal to 3.70 cm^3 K mol^{-1}, which is in the range of values expected for a HS Fe^{2+} ion. As the temperature is lowered below room temperature, $\chi_M T$ first remains constant, then decreases from 240 K down to 210 K, and presents a plateau between 210 and 185 K with $\chi_M T$ = 2.10 cm^3 K mol^{-1} at 200 K; below 185 K, $\chi_M T$ falls very abruptly within a temperature range of 3 K, and eventually is equal to 0.26 cm^3 K mol^{-1} around 30 K. As the temperature is increased, the low-temperature step of the transition is shifted by 3 K toward the high temperatures, while the high-temperature step is unchanged. This behavior reveals a spin conversion occurring in two steps, the low-temperature step being much more abrupt than the high-temperature one, and presenting a thermal hysteresis whose width is 3 K. The inversion temperatures for which 50% of the sites involved in the conversion are HS and 50% are LS may be determined accurately from the extremes of the temperature dependences of the derivatives $d(\chi_M T)/dT$ in both the cooling and warming mode, as shown in Figure 1 (bottom). These inversion temperatures are found as $T_1\uparrow$ = 185 K in the warming mode and $T_1\downarrow$ = 182 K in the cooling mode for the low-temperature step, and T_2 = 222 K for the high-temperature step. The step occurring at low temperature with a thermal hysteresis may be considered as being of the first order.

Calorimetric Measurements

The temperature dependences of the differential scanning calorimeter (DSC) response in both the warming and cooling modes are displayed in Figure 2. As the temperature is lowered, two exothermic peaks are observed, at 188 and 226 K, respectively, the former being much narrower than the latter. As the temperature is increased, the endothermic low-temperature peak occurs at 192 K, and the high-temperature one occurs again at 226 K. The enthalpy and entropy variations are found as ΔH_1 = 5.7 kJ mol^{-1} and ΔS_1 = 30.1 J mol^{-1} K^{-1}, respectively, for the low-temperature step, and as ΔH_2 = 6.5 kJ mol^{-1} and ΔS_2 = 28.6 J mol^{-1} K^{-1}, respectively, for the high-temperature step. Therefore, the total enthalpy and entropy

(41) Varret, F. In *Proceedings of the International Conference on Mössbauer Effect Applications*, Jaipur, India, 1981 (Indian National Science Academy, New Delhi, 1982).

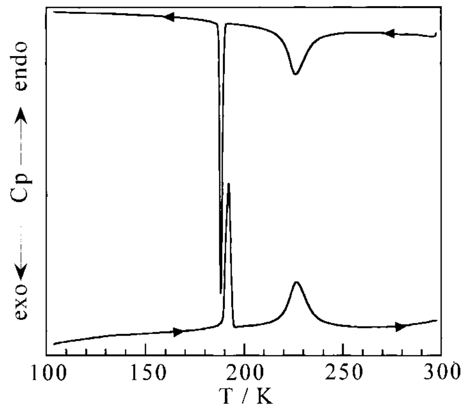

Figure 2. Temperature dependences of the heat capacity for $[Fe(btr)_3](ClO_4)_2$ obtained through differential scanning calorimetry, in both the cooling and warming modes.

variations are found as ΔH = 12.2(1) kJ mol^{-1} and ΔS = 58.8(1) J mol^{-1} K^{-1}, respectively. The total entropy variation is close to the values found for the cooperative spin transition chain compounds $[Fe(NH_2trz)_3](CH_3SO_3)_2{\cdot}H_2O$, 60 J mol^{-1} K^{-1},[27] and $[Fe(NH_2trz)_3](NO_3)_2$, 66 J mol^{-1} K^{-1}, where NH_2-trz stands for 4-amino-1,2,4-triazole.[42] On the other hand, it is lower than the value found for the cooperative two-dimensional compound $[Fe(btr)_2(NCS)_2]{\cdot}H_2O$, 76.4 J mol^{-1} K^{-1}.[43] The experimentally measured entropy variation accounts for an electronic contribution, Rln5 = 13.4 J mol^{-1} K^{-1}, and a dominant vibrational contribution.[3]

Description of the Structure at 260, 190, and 150 K

The structure of the compound was solved at three temperatures, namely, 260 K, where all the Fe^{2+} ions are in the HS state; 190 K, on the plateau between the two steps of the spin conversion; and 150 K, where all the Fe^{2+} ions are in the LS state. The same space group, $R\bar{3}$, is retained at the three temperatures; there is no crystallographic phase transition.

Structure at 260 K. The structure reveals two crystallographically independent iron sites, denoted Fe1 and Fe2. Both the Fe1 and Fe2 sites are located on a 3-fold symmetry axis as well as on an inversion center. Each site is surrounded by six nitrogen atoms occupying the 1- or 1′-positions of six btr ligands. The Fe1−N bond lengths are equal to 2.161(3) Å, and the N−Fe1−N bond angles are equal to 90.8(1)° and 89.2(1)°. The Fe2−N bond lengths are equal to 2.164(3) Å, and the N−Fe2−N bond angles are equal to 88.5(1)° and 91.5(1)°. The Fe2 site is slightly more distorted than the Fe1 site, both in the HS state.

The structure is three-dimensional. Each Fe1 site is bridged to six Fe2 sites through the bis-triazole ligands, with Fe1−Fe2 separations equal to 8.67 Å. The dihedral angle between the mean planes of the two triazole rings within a bis-triazole ligand is equal to 77.35°, which is significantly smaller than the value close to 90° found for the free ligand.[33] The environment of an Fe1 site in the *ab* plane perpendicular to the 3-fold axis is shown in Figure 3. Similarly, each Fe2 site is bridged to six Fe1 sites through the btr ligands. A projection of the structure in the *ac* plane is shown in Figure 4.

(42) (a) Lavrenova, L. G.; Ikorskii, V. N.; Varnek, V. A.; Beresovskii, G. A.; Bessergenev, V. G.; Bausk, N. V.; Erenburg, S. V.; Larionov, S. V. *Koord. Khim.* **1996**, *22* (5), 357. (b) Bessergenev, V. G.; Beresovskii, G. A.; Lavrenova, L. G.; Larionov, S. V. *Zh. Fiz. Khim.* **1997**, *71* (5), 809.
(43) Martin, J. P.; Zarembowitch, J.; Dworkin, A.; Haasnoot, J. G.; Codjovi, E. C. *Inorg. Chem.* **1994**, *33*, 2617.

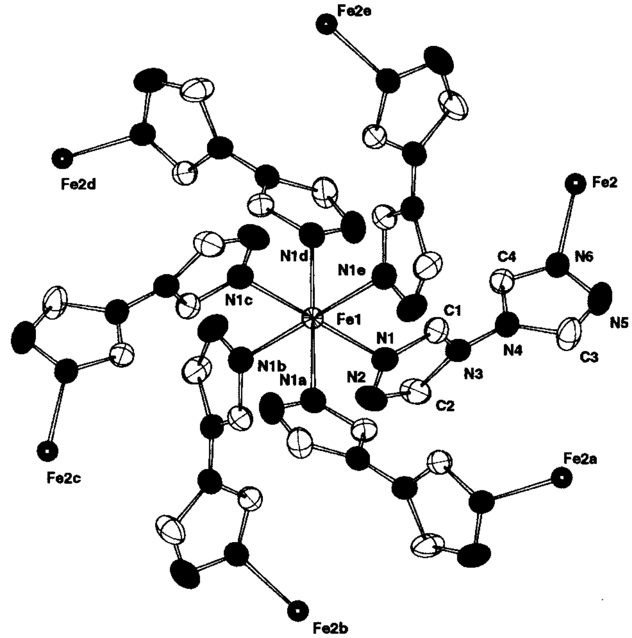

Figure 3. View of the Fe1 site and of its environment in the *ab* plane perpendicular to the 3-fold axis. The hydrogen atoms and the perchlorate anions are omitted for clarity. The symmetry codes are the following. a: $x - y$, $x - z$. b: y, $-x + y$, $-z$. c: $-y$, $x - y - 1$, z. d: $y + {}^2/_3$, $-x + y + {}^1/_3$, $-z + {}^1/_3$. e: $-x + y + 1$, $-x + 1$, z.

There are two crystallographically independent perchlorate anions, located in the voids of the three-dimensional architecture (see Figure 5). These anions show several hydrogen contacts with the carbon atoms of the 1,2,4-triazole rings. Information on the hydrogen contacts is given in Table 3. Two kinds of electrostatic interactions between iron sites and perchlorate anions can be observed, the short ones involving the Fe−N−C−H···O pathway, and the long ones involving the Fe−N−N−C−H···O pathway. The crucial point as far as the existence of a two-step spin conversion is concerned is that the ligand field experienced by the two iron sites is not strictly the same as a result of these weak interactions with the perchlorate anions.

To sum up the structure at 260 K, we can say that the coordination spheres of the two iron sites are typical of Fe^{2+} ions in the HS state.

Structure at 190 K. The $R\bar{3}$ space group is retained, but the volume of the unit cell is 3.3% smaller than at 260 K. The FeN_6 core involving the Fe1 site is very weakly modified. The Fe1−N bond length is equal to 2.151(3) Å, instead of 2.161(3) Å at 260 K, and the N−Fe1−N bond angles are unchanged. On the other hand, the FeN_6 core involving the Fe2 site is strongly modified, being closer to a regular octahedron. The Fe2−N bond length is then equal to 2.007(3) Å, instead of 2.164(3) Å at 260 K, and the bond angles are equal to 89.1(1)° and 90.9(1)°. The Fe1−Fe2 separation through a btr ligand is equal to 8.55 Å, i.e., 0.12 Å shorter than at 260 K. The dihedral angle between the two 1,2,4-triazole moieties of a btr ligand is slightly increased, from 77.35° at 260 K to 79.72° at 190 K.

The coordination sphere of the Fe1 site remains characteristic of an Fe^{2+} ion in the HS state, while that of the Fe2 site with bond lengths close to 2 Å is now characteristic of an Fe^{2+} ion in the LS state.

Structure at 150 K. The decrease in the volume of the unit cell is 2.86% with regard to 190 K, and 6% with regard to 260 K. The main structural modification between 190 and 150 K concerns the coordination sphere of the Fe1 site. The Fe1−N bond length is now equal to 1.987(5) Å, and the N−Fe1−N

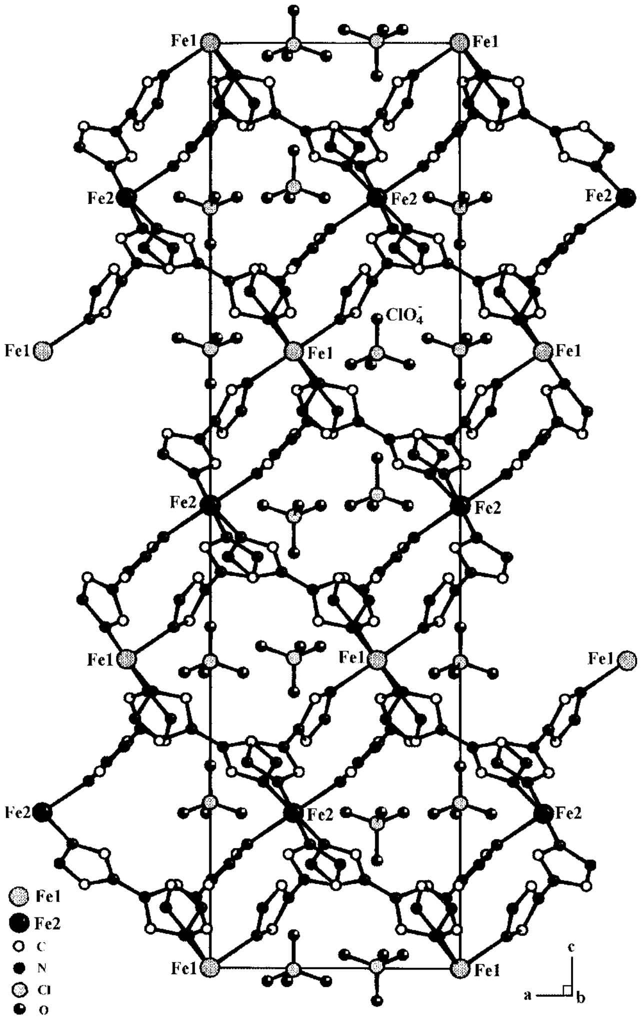

Figure 4. Projection of the crystal structure of $[Fe(btr)_3](ClO_4)_2$ in the *ac* plane. The hydrogen atoms are omitted for clarity.

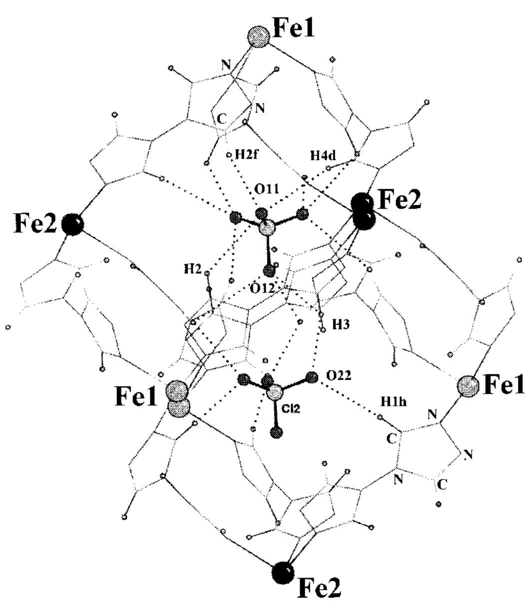

Figure 5. View of the hydrogen bonds between the perchlorate anions and the triazole rings, and of the Fe−N−CH···O and Fe−N−N−CH···O interactions for $[Fe(btr)_3](ClO_4)_2$.

bond angles are very close to the 90° value for a regular octahedron; they are equal to 89.9(2)° and 90.1(2)°. The Fe2−N bond length is equal to 1.994(5) Å, and surprisingly the $Fe2N_6$ octahedron is slightly more distorted than at 190 K, with N−Fe2−N bond angles of 88.6(2)° and 91.4(2)°. The distortion with respect to a regular octahedron of the LS Fe2 site at 150 K is about the same as that of the HS Fe2 site at 260 K. The Fe1−Fe2 separation through the btr ligand is further reduced by 0.13 Å with regard to 190 K; it is equal to 8.42 Å. The modification of the dihedral angle between the two 1,2,4-triazole moieties of a btr ligand between 190 and 150 K is much more dramatic than between 260 and 190 K. The value of this dihedral angle increases from 79.72° to 87.17° as the temperature is lowered from 190 K down to 150 K. The geometry of the btr ligand at 150 K when the two Fe^{2+} sites are LS is very close to that of the free molecule.[33]

The bond lengths around both the Fe1 and Fe2 sites at 150 K are characteristic of Fe^{2+} ions in the LS state. The evolutions of the bond lengths and angles around the Fe1 and Fe2 sites along with that of the Fe1−Fe2 separation are gathered in Table 2, and the distances and angles involved in the hydrogen contacts between perchlorate anions and 1,2,4-triazole rings are given in Table 3.

Table 2. Evolution of the Fe−N Bond Lengths, N−Fe−N Bond Angles, and Fe1−Fe2 Separations at 260, 190, and 150 K[a]

	T = 260 K	T = 190 K	T = 150 K
Fe1−Fe2	8.67	8.55	8.42
Fe1−N1	2.161(3)	2.151(3)	1.987(5)
Fe2−N6	2.164(3)	2.007(3)	1.994(5)
N1−Fe1−N1[a]	90.8(1)	90.7(1)	89.9(2)
N1−Fe1−N1[b]	89.2(1)	89.3(1)	90.1(2)
N6−Fe2−N6[c]	91.5(1)	90.9(1)	91.4(2)
N6−Fe2−N6[d]	88.5(1)	89.1(1)	88.6(2)
Fe1−N1−N2	122.3(2)	122.7(2)	124.4(4)
Fe1−N1−C1	121.9(2)	121.7(3)	124.4(4)
Fe2−N6−N5	126.8(2)	125.0(2)	125.7(4)
Fe2−N6−C4	123.5(4)	126.0(3)	125.4(4)

[a] The distances are expressed in Å, and the angles in deg. The atoms marked with a letter are generated with the following symmetry operations. a: $x - y, x, -z$. b: $y, -x + y, -z$. c: $-y, x - y - 1, z$. d: $y + {}^2/_3, -x + y + {}^1/_3, -z + {}^1/_3$.

Table 3. Distances (Å) and Angles (deg) Involved in the Hydrogen Bonds between Perchlorate Anions and 1,2,4-Triazole Rings[a]

D−H···A	T (K)	D−H	H···A	D−H···A
	260	0.95(5)	2.69(5)	170.0(36)
C−H(1[h])···O(22)	190	0.95(5)	2.66(5)	171.7(36)
	150	0.93(6)	2.57(6)	167.2(44)
	260	0.96(5)	2.57(6)	164.6(41)
C−H(3)···O(22)	190	0.89(5)	2.61(5)	162.3(41)
	150	0.92(6)	2.55(6)	162.2(50)
	260	0.96(5)	3.04(5)	93.8(33)
C−H(3)···O(12)	190	0.89(5)	2.83(5)	108.4(35)
	150	0.92(6)	2.87(6)	107.4(42)
	260	0.95(5)	2.69(4)	112.7(32)
C−H(2)···O(11)	190	0.97(5)	2.66(5)	108.7(34)
2/3			2.93(8)	96.8(61)
1/3	150	0.81(8)	2.75(8)	107.4(63)
	260	0.95(5)	3.02(5)	135.5(33)
C−H(2[f])···O(11)	190	0.97(5)	2.89(5)	134.1(36)
2/3			2.88(8)	155.5(68)
1/3	150	0.81(8)	2.92(9)	137.4(67)
	260	0.92(5)	3.00(5)	156.9(39)
C−H(4[d])···O(11)	190	0.96(5)	2.82(5)	158.6(37)
2/3			2.51(6)	132.0(46)
1/3	150	1.00(7)	2.92(9)	160.2(47)

[a] The standard deviations are given in parentheses. The atoms marked with a letter are generated with the following symmetry operations. d: $y + {}^2/_3, -x + y + {}^1/_3, -z + {}^1/_3$. f: $-x + {}^2/_3, -y + {}^1/_3, -z + {}^1/_3$. h: $-x + 1, -y, -z$.

Table 4. Representative Least-Squares-Fitted Mössbauer Data for $[Fe(btr)_3](ClO_4)_2$[a]

	HS(1)			HS(2)			LS			
T (K)	δ	ΔE_Q	$\Gamma/2$	δ	ΔE_Q	$\Gamma/2$	δ	ΔE_Q	$\Gamma/2$	A_{HS}/A_{tot} (%)
293	1.008(1)	0.945(1)	0.134(1)							100
270	1.015(1)	1.232(1)	0.120(1)	1.016(1)	0.906(2)	0.120(1)				100
260	1.023(1)	1.347(2)	0.117(1)	1.029(1)	0.937(3)	0.133(1)	0.507(3)	0.200*	0.056(5)	98.60
240	1.023(1)	1.482(3)	0.140(2)	1.044(2)	0.958(3)	0.140(2)	0.456(7)	0.200*	0.089(8)	93.40
230	1.029(1)	1.549(3)	0.133(2)	1.050(2)	0.984(4)	0.133(2)	0.500(8)	0.190*	0.149(8)	84.30
227.5	1.040(1)	1.579(3)	0.134(2)	1.066(3)	0.988(5)	0.134(2)	0.502(6)	0.190*	0.144(6)	77.90
225	1.041(1)	1.588(2)	0.132(1)	1.070(2)	1.005(4)	0.132(1)	0.505(3)	0.190*	0.144(3)	71.80
220	1.045(1)	1.608(2)	0.127(1)	1.09(2)	1.00(3)	0.15(5)	0.503(4)	0.187(8)	0.133(2)	59.70
215	1.048(1)	1.628(1)	0.130(1)	1.1(1)	0.9(2)	0.129(9)	0.50(1)	0.19(2)	0.131(1)	53.40
200	1.057(1)	1.730(1)	0.127(1)				0.510(1)	0.199(1)	0.123(1)	50.40
187	1.067(1)	1.826(1)	0.128(1)				0.509(1)	0.199(1)	0.126(1)	45.10
186.6	1.062(1)	1.820(2)	0.125(1)				0.512(1)	0.203(1)	0.130(1)	40.60
186.4	1.063(1)	1.816(1)	0.127(1)				0.510(1)	0.199(1)	0.126(1)	34.90
185.8	1.061(1)	1.809(2)	0.128(2)				0.510(1)	0.198(1)	0.128(1)	30.60
185.1	1.066(1)	1.813(2)	0.129(2)				0.508(1)	0.196(1)	0.123(1)	26.70
184.2	1.062(2)	1.804(4)	0.143(3)				0.511(1)	0.198(1)	0.126(1)	20.30
183.6	1.065*	1.8*	0.158(9)				0.511(1)	0.199(1)	0.128(1)	9.20
182	1.059*	1.8*	0.17(2)				0.512(1)	0.199(1)	0.125(1)	6.10
175	1.059*	1.8*	0.21(3)				0.510(1)	0.197(1)	0.128(1)	3.50
160	1.059*	1.8*	0.19(5)				0.516(1)	0.195(1)	0.131(1)	1.82
140	1.059*	1.8*	0.250				0.513(1)	0.191(1)	0.129(1)	0.51
120							0.522(1)	0.193(1)	0.13(1)	0
80							0.530(1)	0.190(1)	0.136(1)	0

[a] Isomer shifts (δ) refer to metallic iron at room temperature (1 mm s^{-1} = 1.12 × 10^7 s^{-1}); ΔE_Q = quadrupole splitting (mm s^{-1}); $\Gamma/2$ = half-width of the lines (mm s^{-1}); statistical standard deviations are given in parentheses; values marked with an asterisk (*) were fixed for the fit.

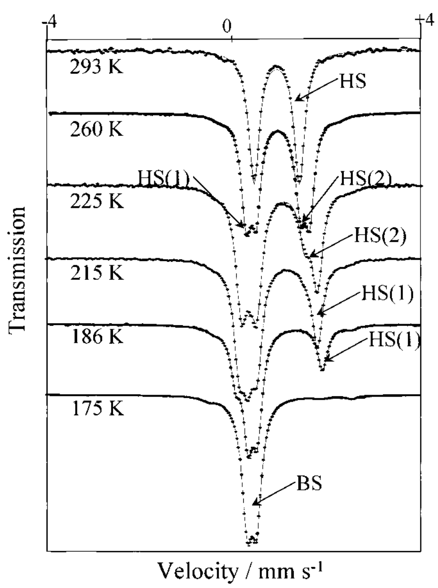

Figure 6. Selected Mössbauer spectra for $[Fe(btr)_3](ClO_4)_2$.

Mössbauer Spectroscopy

The two-step spin conversion was also investigated by Mössbauer spectroscopy, which allows us to follow the temperature dependence of the HS and LS molar fractions in an accurate way.[44] The spectra were recorded in the cooling mode. Some representative spectra are shown in Figure 6, and selected values of the Mössbauer parameters obtained by least-squares fitting of the experimental data are gathered in Table 4.

At room temperature, the spectrum consists of a unique quadrupole split doublet, with an isomer shift δ = 1.008(1) mm s^{-1} and a quadrupole splitting ΔE_Q = 0.945(1) mm s^{-1}. These two parameters are typical of a HS Fe^{2+} ion. At 270 K, a splitting of this doublet into two distinct quadrupole split doublets is observed, with parameters δ = 1.015(1) mm s^{-1} and ΔE_Q = 1.232(1) mm s^{-1}, and δ = 1.016(1) mm s^{-1} and ΔE_Q = 0.906(2) mm s^{-1}, respectively. These two HS doublets, which are well distinguished on the spectrum at 260 K of Figure 6, are noted HS(1) and HS(2), the quadrupole splitting of the former being larger than that of the latter. Below 270 K, another doublet appears, corresponding to a LS Fe^{2+} ion; its parameters at 220 K are δ = 0.503(4) mm s^{-1} and ΔE_Q = 0.187(8) mm s^{-1}. At 225 K, the intensity of HS(2) is reduced by a factor of 2, which indicates that HS(2) is associated with the Fe2 site in the HS state. At 200 K, the spectrum consists of HS(1) associated with the Fe1 site in the HS state along with the LS doublet mentioned above. As the temperature is lowered further, the intensity of the LS doublet increases at the expense of that of HS(1), and below 140 K, only this LS doublet is detectable. The Mössbauer spectroscopy does not distinguish the two LS sites detected by X-ray diffraction.

The high-temperature (T > 260 K) and low-temperature (T < 140 K) spectra evidence the absence of residual LS and HS fraction, respectively. At each temperature, the high-spin molar fraction, x_{HS}, may be deduced from the area ratio A_{HS}/A_{tot} determined from the least-squares fitting of the spectra. The x_{HS} versus T curve represented in Figure 7 confirms the occurrence of a two-step spin conversion with a ca. 20 K plateau where an almost perfect spin-state equilibrium involving 50% of HS and LS molecules is retained. This curve confirms the results deduced from the magnetic data. The high-temperature step, centered at 226 K, is rather gradual while the low-temperature step, centered at 185 K, is very abrupt.

Discussion

The two main findings of this work are the three-dimensional character of the crystal structure and the occurrence of a two-step spin conversion with a plateau of ca. 20 K between these two steps. We would like to discuss both aspects.

Let us begin with some structural considerations. The ligand btr was already utilized to obtain extended networks. In all of

(44) Gütlich, P.; Link, R.; Trautwein, A. In *Mössbauer Spectroscopy and Transition Metal Chemistry*; Springer: Berlin, 1978.

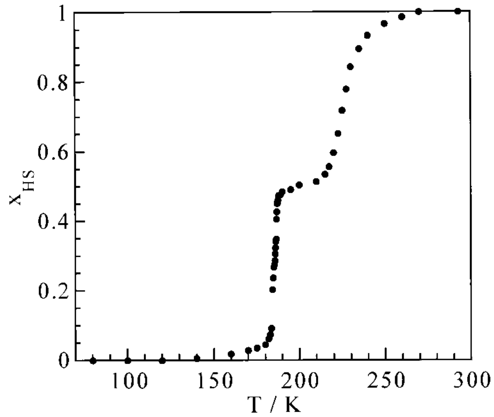

Figure 7. Temperature dependence of the high-spin molar fraction for $[Fe(btr)_3](ClO_4)_2$, as deduced from the Mössbauer spectra.

the cases, it bridges two metal ions through the nitrogen atoms occupying the 1- and 1′-positions, with metal−metal separations of the order of 9 Å.[45] When coordinating anions, such as NCS^-, are also present, one- or two-dimensional species are obtained.[18,19,46−49] For instance, $[Fe(btr)_2(NCS)_2]\cdot H_2O$ is a two-dimensional spin crossover compound exhibiting a well-pronounced thermal hysteresis loop with inversion temperatures found as $T\uparrow = 145$ K in the warming mode and $T\downarrow = 121$ K in the cooling mode.[18] Interestingly, when the noncoordinated water molecule is released, the spin conversion is suppressed; the compound is HS in the whole temperature range. In the absence of coordinating anions, three-dimensional species were obtained. This is the case for the compound $[Co(btr)_3](CF_3SO_3)_2$. Unfortunately, the crystal structure of this compound has not been properly refined. In particular, the triflate anions have not been located.[49]

Another three-dimensional Fe^{2+} compound with a bis-triazole ligand has been reported. Its formula is $[Fe(bte)_3](BF_4)_2$ with bte = 1,2-bis(1,2,4-triazole-1-yl)ethane. Its structure has also been refined in the $R\bar{3}$ space group. However, no spin conversion was observed. The compound is HS down to very low temperature.[50]

Let us now consider the occurrence of two-step spin conversions. The very first compound for which a two-step spin conversion was observed is $[Fe(2\text{-pic})_3]Cl_2\cdot EtOH$, with 2-pic = 2-picolylamine.[51] In this compound, there is a unique iron crystallographic site, and consequently the two-step conversion has not the same origin as for $[Fe(btr)_3](ClO_4)_2$.[52] It has been attributed to a competition between long-range cooperative and short-range anticooperative interactions.[53] Doping $[Fe(2\text{-pic})_3]Cl_2\cdot EtOH$ with a small amount (10%) of Zn^{2+} or applying a weak (1 kbar) external pressure results in the merging of the two steps.[54] Other two-step transitions in Fe^{2+} mononuclear compounds were afterward described. It is in particular the case for Fe[5-NO_2-sal-N(1,4,7,10)], where 5-NO_2-sal-N(1,4,7,10) is a hexadentate ligand arising from the Schiff base condensation of 5-NO_2-salicylaldehyde with 1,4,7,10-tetraazadecane. In this compound, the two-step conversion is associated with structural phase transitions evidenced by X-ray diffraction studies at three temperatures.[55] Again, the mechanism of the two-step conversion has been ascribed to a competition between long-range cooperative and short-range anticooperative interactions, and therefore is not the same as for the title compound. A two-step transition was also observed in the binuclear compound $[Fe(bt)(NCS)_2]_2$bpym, with bt = 2,2′-bi-2-thiazoline and bpym = 2,2′-bipyrimidine.[56] The crystal structure of the compound could not be determined, and the occurrence of two steps was attributed to a synergistic effect between intramolecular interactions favoring the mixed-spin state and intermolecular interactions favoring like-spin species domains. It is worth mentioning that, for $[Fe(bt)(NCS)_2]_2$bpym, the low-temperature step is also more abrupt than the high-temperature one.

Two Fe^{2+} crystallographic sites were also found for $[Fe(mtz)_6]X_2$, with mtz = 1-methyltetrazole, and $X^- = ClO_4^-$ or BF_4^-.[57] One of the sites undergoes a spin transition around 100 K, while the other remains HS in the whole temperature range.[58−60] An analogous situation was observed for $[Fe(etz)_6]X_2$, with etz = 1-ethyltetrazole, except that the proportions are 1/3 for the HS site and 2/3 for the spin transition site,[61] instead of 1/2 for both sites of $[Fe(mtz)_6]X_2$.

For $[Fe(btr)_3](ClO_4)_2$, the two steps of the spin conversion are associated with the presence of two Fe^{2+} crystallographically independent sites, denoted Fe1 and Fe2. These two sites are very close to each other from a structural viewpoint. Each of them is located on a 3-fold symmetry axis as well as on an inversion center; Fe1 is surrounded by six−btr−Fe2 linkages, and Fe2 is surrounded by six−btr−Fe1 linkages. The slight difference between Fe1 and Fe2 arises from the differences in interactions between these sites and the noncoordinated perchlorate anions through the weak Fe−N−C−H···$OClO_3$ and Fe−N−N−C−H···$OClO_3$ hydrogen contacts. In other terms, the six perchlorate anions surrounding an Fe1 site do not electrostatically interact with this site in the same way as the six perchlorate anions surrounding an Fe2 site do.

The high-temperature step, centered around $T_2 = 222$ K, corresponds to the LS ↔ HS transition for the Fe2 site. This step is not very abrupt and occurs without thermal hysteresis. The low-temperature step, centered around $T_1 = 185$ K, corresponds to the LS ↔ HS transition for the Fe1 site. This step is much more abrupt and occurs with a thermal hysteresis whose width is about 3 K. Between T_1 and T_2, the structure of the material is rather peculiar. Each LS Fe2 site is surrounded by six HS Fe1 sites, and similarly each HS Fe1 site is surrounded by six LS Fe2 sites. As far as the difference of abruptness between steps 1 and 2 of the spin conversion is concerned, it

(45) Haasnoot, J. G. In *Magnetism: A Supramolecular Function*; Kahn, O. Ed.; Kluwer: Dordrecht, The Netherlands, 1996; p 299.
(46) Biagini-Cingi, M.; Manotti-Lanfredi, A. M.; Ugozzoli, F.; Haasnoot, J. G.; Reedijk, J. *Gazz. Chim. Ital.* **1994**, *124*, 509.
(47) Vreugdenhil, W.; Haasnoot, J. G.; De Graaff, R. A. G.; Nieuwenhuis, H. A.; Reefman, D.; Reedijk, J. *Acta Crystallogr.* **1987**, *C43*, 1527
(48) Vreugdenhil, W.; Gorter, S.; Haasnoot, J. G.; Reedijk, J. *Polyhedron* **1985**, *4*, 1769.
(49) Vreugdenhil, W. Ph.D. Thesis, Leiden University, The Netherlands, 1987.
(50) Kolnaar, J. J. A.; Guijt, R. C.; Haasnoot, J. G.; Smeets, W. J. J.; Spek, A. L.; Reedijk, J. *Angew. Chem., Int. Ed.*, in press.
(51) Köppen, H.; Müller, E. N.; Köhler, C. P.; Spiering, H.; Meissner, E.; Gütlich, P. *Chem. Phys. Lett.* **1982**, *91*, 348.
(52) Mikami, M.; Konno, M.; Saito, Y. *Chem. Phys. Lett.* **1979**, *63*, 566.
(53) Jakobi, R.; Spiering, H.; Gütlich, P. *J. Phys. Chem. Solids* **1992**, *53*, 267.
(54) Köhler, C. P.; Jacobi, R.; Meissneir, E.; Wiehl, L.; Spiering, H.; Gütlich, P. *J. Phys. Chem. Solids* **1990**, *51*, 239.
(55) Boinnard, D.; Bousseskou, A.; Dworkin, A.; Savariault, J. M.; Varret, F.; Tuchagues, J. P. *Inorg. Chem.* **1994**, *33*, 271.
(56) Real, J. A.; Bolvin, H.; Bousseskou, A.; Dworkin, A.; Kahn, O.; Varret, F.; Zarembowitch, J. *J. Am. Chem. Soc.* **1992**, *114*, 4650.
(57) Wiehl, L. *Acta Crystallogr.* **1993**, *B49*, 289.
(58) Poganiuch, P.; Decurtins, S.; Gütlich, P. *J. Am. Chem. Soc.* **1990**, *112*, 3270.
(59) Poganiuch, P.; Gütlich, P. *Hyperfine Interact.* **1988**, *40*, 331.
(60) Buchen, T.; Poganiuch, P.; Gütlich, P. *J. Chem. Soc., Dalton Trans.* **1994**, 2285.
(61) Hinek, R.; Spiering, H.; Schollmeyer, D.; Gütlich, P.; Hauser, A. *Chem.*−*Eur. J.* **1996**, *2*, 1127.

can be pointed out that the LS $\leftrightarrow$ HS conversion for the Fe1 site around T_1 is accompanied by a dramatic modification of the geometry of the btr bridge. This is in contrast with the LS $\leftrightarrow$ HS conversion of the Fe2 site around T_2 which is accompanied by a weak modification of the geometry of the btr bridge. There is an obvious correlation between the difference of steepness for steps 1 and 2 on one hand and the structural modifications accompanying these steps on the other hand. Despite the pronounced structural modifications accompanying step 1, the $R\bar{3}$ space group is retained. These observations illustrate that a first-order spin transition is accompanied by structural modifications extending well beyond the metal coordination sphere even when it is not associated with a crystallographic phase transition.

The three-dimensional architecture characterized for $[Fe(btr)_3](ClO_4)_2$ seems to be very versatile in terms of occurrence of spin conversion. The perturbation created by the noncoordinating anions plays a key role in the spin conversion regime. A two-step conversion is observed for the title compound. Replacing ClO_4^- by BF_4^- results in a material in which only one of the Fe^{2+} sites undergoes a spin conversion, the other one remaining HS in the whole temperature range.[62] Finally, using $CF_3SO_3^-$ as a counteranion results in a HS material.[45,49] We intend to investigate further the control of the spin conversion regime through the nature of the counteranion inserted in the voids of the three-dimensional architecture.

Acknowledgment. This work was partly funded by the TMR Research Network ERB-FMRX-CT98-0199 entitled “Thermal and Optical Switching of Molecular Spin States (TOSS)”.

Supporting Information Available: Tables of X-ray crystallographic data for $[Fe(btr)_3](ClO_4)_2$. This material is available free of charge via the Internet at http://pubs.acs.org.

IC990511Q

(62) Garcia, Y.; Kahn, O. Unpublished result.